



ORIGINAL ARTICLE OPEN ACCESS

Molecular Characterisation of the Peroxidase Gene Family in *Botrytis cinerea* and the Role of BcPRD7 in Virulence

Shixuan Zhang^{1,2} | Jialin Wang^{2,3} | Bai Li^{3,4} | Jinping Zang^{1,2} | Hongzhe Cao^{1,2}  | Jihong Xing^{1,2,3} | Jingao Dong^{1,3,4} | Kang Zhang^{1,2,3} 

¹State Key Laboratory of North China Crop Improvement and Regulation, Hebei Agricultural University, Baoding, China | ²Hebei Key Laboratory of Plant Physiology and Molecular Pathology, Hebei Agricultural University, Baoding, China | ³College of Life Sciences, Hebei Agricultural University, Baoding, China | ⁴College of Plant Protection, Hebei Agricultural University, Baoding, China

Correspondence: Kang Zhang (zk7588@163.com) | Jihong Xing (xingjihong2000@126.com)

Received: 20 December 2024 | **Revised:** 30 January 2025 | **Accepted:** 25 February 2025

Funding: This study was supported by the Science & Technology Program of Hebei, 23567601H, National Natural Science Foundation of China, 32072369; Natural Science Foundation of Hebei Province, C2022204040; Research Project of Science and Technology in Colleges and Universities of Hebei Province, BJ2022006; Baoding Science and Technology Project Program, 2472P005.

Keywords: BcHEX | BcPRD7 | *Botrytis cinerea* | growth and development | pathogenicity | peroxidase | stress

ABSTRACT

Peroxidase activity is essential for the virulence of a number of plant-pathogenic fungi. However, there are few reports of the systematic analysis of peroxidase genes in *Botrytis cinerea*. We identified all the peroxidase genes of *B. cinerea* by searching the fungal peroxidase database and found that the expression levels of *BcPRD3*, *BcPRD7*, *BcPRD8* and *BcPRD10* changed significantly during hyphal development and in response to H₂O₂ stress treatment and infection of *Arabidopsis thaliana* by *B. cinerea*. We found that the hyphae of the mutant strains became more slender, the number and size of the infection structures decreased, the number of conidia decreased and the stress response and virulence decreased significantly. These four genes positively regulated the growth, development and pathogenicity of *B. cinerea* and participated in osmotic and oxidative stress response and cell integrity maintenance. In addition, we also found that *BcPRD7* played important roles in oxidase enzyme activity, ion penetration, the synthesis and metabolism of mycotoxins, and determined the interaction between *BcPRD7* and *BcHEX*, the latter being the major protein of the Woronin body. It is speculated that *BcPRD7* may regulate the growth, development and pathogenicity of the pathogen by participating in the development of the Woronin body. The function of peroxidase family genes in *B. cinerea* was systematically analysed in this study, which provides a solid foundation for the subsequent in-depth elucidation of the relevant regulatory mechanisms and is expected to provide new ideas and strategies for the prevention and control of *B. cinerea* diseases.

1 | Introduction

Botrytis cinerea is one of the 10 most economically destructive plant pathogens, causing grey mould in thousands of plant species and posing a serious threat to the economic value of these crops (Dean et al. 2012). *B. cinerea* usually infects dicotyledonous plants and begins to infect at the early stage of crop growth and rapidly spreads under conducive conditions to cause crop

disease. Also, there is a risk to mature (senescing) fruits like strawberry fruits. Infection by *B. cinerea* is mainly caused by conidia adhering to and germinating on the surface of plants. It has been reported that *B. cinerea* can directly enter the host through stomata or directly penetrate the plant cuticle through conidial germ tubes (Glazebrook 2005). In the early stage of infection, conidia germinate and form the initial infection site. At this stage, the fungus mainly stays on the host surface and kills the host

Shixuan Zhang and Jialin Wang contributed equally to this work.

This is an open access article under the terms of the [Creative Commons Attribution-NonCommercial-NoDerivs](https://creativecommons.org/licenses/by-nc-nd/4.0/) License, which permits use and distribution in any medium, provided the original work is properly cited, the use is non-commercial and no modifications or adaptations are made.

© 2025 The Author(s). *Molecular Plant Pathology* published by British Society for Plant Pathology and John Wiley & Sons Ltd.

cells with the help of cell-wall hydrolytic proteins (Stefanato et al. 2009; You and van Kan 2021). In the middle stage of infection, *B. cinerea* proliferates in dead plant tissues, forms superficial hyphae, and differentiates into appressoria and infection cushions (multicellular appressoria dedicated to plant penetration), which help *B. cinerea* penetrate the host tissues. Infection cushions produce many virulence factors to help the pathogen penetrate and colonise the host plant. All pathways lead to the local accumulation of fungal biomass at the site of infection, resulting in a greater area of infection in the host (Bi et al. 2023). In the late stage of infection, *B. cinerea* destroys the cuticle and cell wall of host plants and induces plants to produce defence compounds that resist the infection of pathogenic fungi. At the same time, *B. cinerea* can resist such toxic antifungal metabolites from plants by, for example, the degradation of α -tomatine and the generation of toxic glucosinolate degradation products (Piasecka et al. 2015; Vela-Corcía et al. 2019). Grey mould can also cause huge economic post-harvest losses during transportation and storage (Staats et al. 2005; Williamson et al. 2007). Therefore, it is of considerable commercial significance to explore the pathogenic mechanism of *B. cinerea*.

The processes involved in the production and elimination of reactive oxygen species (ROS) play an important role in the interaction between pathogens and plants. The oxidative burst in plants caused by infection by plant-pathogenic fungi is characterised by local ROS accumulation. Therefore, the successful removal of plant-derived ROS by pathogenic fungi is essential for their survival and virulence. Therefore, pathogen proteins that contribute to ROS catabolism and affect cell oxidation, such as oxidoreductases, are potential virulence factors. Studies have shown that *B. cinerea* secretes a cytochrome c peroxidase that promotes plant invasion by detoxifying host-derived ROS (Yang et al. 2022).

Peroxidases play an important role in reducing levels of ROS and protecting macromolecules such as proteins and lipids from oxidation. Peroxidases are mainly present in the peroxisomes, where they represent the core enzyme activity. Peroxisomes can adjust their shape, size, location and abundance in response to changes in nutritional or environmental conditions (Lodhi and Semenkovich 2014). The dynamic processes of the formation and dissolution of peroxisomes maintain the homeostasis of peroxisome functions in fungi (Mahalingam et al. 2021). Removal of redundant or dysfunctional peroxisomes helps to maintain peroxisome function and prevents the accumulation of damaged peroxisomes during cell senescence (Platta and Erdmann 2007), with new peroxisomes being formed by the division or regeneration of pre-existing peroxisomes (He et al. 2021).

As marker enzymes of peroxisomes, peroxidases are widely distributed in plants, animals and microorganisms. In plants, inhibition of peroxidase activity in *Arabidopsis* can alter cell wall and phenylpropanoid metabolism (Shigeto et al. 2013). It has been reported that the peroxidase activity of *Chrysanthemum* increases sharply in response to drought stress, helping plants to tolerate drought by scavenging more ROS (Hodaei et al. 2018). In *Capsicum* seedlings, saline-alkali stress greatly inhibits seedling growth and reduces the plant growth rate; by applying regulators to enhance the redox metabolic pathway of peroxidases, the saline-alkali tolerance of *Capsicum* seedlings was greatly

improved (Wang et al. 2024). In animals, the biological activity of heme peroxidase is related to antifungal and antiviral functions (Octavia et al. 2012), and abnormal peroxidase activity is associated with diseases such as myocardial infarction, asthma and Alzheimer's disease. In mosquitoes, an imbalance in the antioxidant defence system has adverse effects on male fertility and reproductive physiology (Shaw et al. 2014). Studies have shown that heme peroxidase is an important cytokine that protects sperm from oxidative stress and maintains semen quality in the reproductive organs of male mosquitoes, thus directly affecting the mosquito population (Chen et al. 2021).

In microorganisms, peroxidases are essential for the virulence of a range of phytopathogenic fungi. In a report on *Magnaporthe oryzae*, the causative organism of rice blast disease, peroxidase activity significantly affected the virulence of the fungus (Heller and Tudzynski 2011). A knockout mutant of *MoPRX1* was constructed, and the response to stress by and virulence analysis of the mutant showed that *MoPRX1* activity of rice blast was positively correlated with H_2O_2 stress tolerance and virulence (Auh and Murphy 1995). With the help of electron donors, peroxidases exhibited antioxidant function in *M. oryzae* (Shai et al. 2018) and then regulated its virulence and asexual reproduction process (Wang et al. 2013). *Fusarium graminearum* is a filamentous fungal pathogen that can cause Fusarium wilt of wheat. The peroxidase gene *FgNoxR* in *F. graminearum* was identified and found to play an important role in its virulence. *FgNoxR* is localised on punctate structures throughout the cytoplasm in aerial hyphae; these structures tend to accumulate at or near the plasma membrane, septum and hyphal tip of germinated conidia. Deletion of the *FgNoxR* gene led to decreases in conidium formation and germination, which affected the virulence (Torres et al. 2002; Lee et al. 2018, 2020). In *Penicillium chrysogenum*, it was found that a peroxidase is involved in the biosynthesis of penicillin through the action of peroxisomes. Overexpression of the *PcPEXP* gene led to a proliferation of tubular microsomes, which increased penicillin production by *P. chrysogenum* (Kiel et al. 2005); penicillin production could increase 2–2.5 times using this strategy.

However, few systematic studies on the peroxidase gene family in *B. cinerea* have been published. We aim to use bioinformatic methods to analyse and functionally characterize the peroxidase gene families of *B. cinerea*. At the same time, by constructing mutants of key genes, the functions of the peroxidase family of *B. cinerea* in the growth, development and virulence of this pathogen could be further explored, which provides a baseline for the study of the function and regulatory mechanism of the peroxidase gene family of *B. cinerea* and could form a theoretical basis for the prevention and control of grey mould.

2 | Results

2.1 | Identification, Phylogenetic Evolution and Chromosome Mapping Analysis of the Peroxidase Gene Family in *B. cinerea*

We used bioinformatic methods to perform phylogenetic analysis of the peroxidase family genes in *B. cinerea*, *M. oryzae* and *Saccharomyces cerevisiae*. After analysis, the sequences of 31

TABLE 1 | Physicochemical properties of peroxidase family genes in *Botrytis cinerea*.

Gene name	Gene ID	Chromosome	Start codon	Stop codon	CDS	AA	MW (kDa)	pI
<i>BcNOXR</i>	<i>BC1G_06200</i>	Chr3	2,311,352	2,315,090	1623	540	61.26	5.80
<i>BcGPX3</i>	<i>BC1G_02031</i>	Chr3	492,223	494,220	765	254	19.36	5.95
<i>BcPRX4</i>	<i>BC1G_00059</i>	Chr1	2,968,621	2,969,951	690	229	25.58	6.10
<i>BcPRX3</i>	<i>BC1G_06262</i>	Chr16	131,243	132,750	792	263	22.48	9.23
<i>BcPRX1</i>	<i>BC1G_07040</i>	Chr4	214,534	216,674	1050	349	36.22	7.54
<i>BcCCP1</i>	<i>BC1G_08301</i>	Chr1	3,254,960	3,257,185	1119	372	40.76	8.50
<i>BcCCP2</i>	<i>BC1G_11611</i>	Chr7	2,149,013	2,150,624	882	293	34.42	6.10
<i>BcPRD11</i>	<i>BC1G_04955</i>	Chr13	1,279,863	1,288,816	1614	537	57.91	4.48
<i>BcPRD10</i>	<i>BC1G_14974</i>	Chr3	2,680,257	2,682,916	1608	535	53.87	4.66
<i>BcPRX7</i>	<i>BC1G_13939</i>	Chr2	2,995,918	2,997,499	543	180	20.56	8.69
<i>BcPRX9</i>	<i>BC1G_05133</i>	Chr10	419,238	421,031	471	156	16.31	5.33
<i>BcPRX8</i>	<i>BC1G_09932</i>	Chr9	1,393,182	1,394,631	720	239	18.18	5.20
<i>BcPRD1</i>	<i>BC1G_06374</i>	Chr13	2,164,260	2,166,607	1542	513	53.78	6.43
<i>BcPPOA70</i>	<i>BC1G_08479</i>	Chr14	839,453	840,529	600	199	22.15	5.46
<i>BcPRD7</i>	<i>BC1G_04705</i>	Chr10	976,618	978,809	831	276	30.69	5.64
<i>BcPRD3</i>	<i>BC1G_03406</i>	Chr11	1,465,875	1,467,075	834	277	29.92	4.59
<i>BcPRD6</i>	<i>BC1G_11384</i>	Chr2	2,228,343	2,229,971	951	316	35.61	5.60
<i>BcPRD8</i>	<i>BC1G_01628</i>	Chr5	896,444	868,576	1329	442	47.31	4.61
<i>BcPRD2</i>	<i>BC1G_12449</i>	Chr5	573,177	575,869	1302	433	46.30	5.88
<i>BcPRD4</i>	<i>BC1G_09364</i>	Chr5	223,653	225,647	1311	436	47.18	4.88
<i>BcPRD5</i>	<i>BC1G_12525</i>	Chr3	108,776	110,693	1284	427	45.84	5.11
<i>BcPRD9</i>	<i>BC1G_09959</i>	Chr9	1,337,227	1,338,806	1248	415	43.33	4.76
<i>BcPPOA90</i>	<i>BC1G_04254</i>	Chr4	1,724,037	1,728,750	3462	1153	126.17	6.19
<i>BcppoA80</i>	<i>BC1G_14780</i>	Chr2	1,097,131	1,102,185	3858	1286	136.49	6.11
<i>BcNOXA</i>	<i>BC1G_10823</i>	Chr5	143,183	147,870	1662	553	63.42	8.04
<i>BcCAT2</i>	<i>BC1G_12856</i>	Chr11	2,289,386	2,291,960	2145	714	61.05	5.51
<i>BcCAT3</i>	<i>BC1G_02407</i>	Chr6	1,539,352	1,542,118	2214	737	82.10	5.91
<i>BcCAT6</i>	<i>BC1G_13021</i>	Chr5	1,624,387	1,626,743	1506	501	55.56	6.53
<i>BcCATA</i>	<i>BC1G_01095</i>	Chr6	430,726	432,971	1626	541	60.68	6.18
<i>BcCAT4</i>	<i>BC1G_09386</i>	Chr5	292,260	294,217	1692	563	63.86	6.23
<i>BcCAT5</i>	<i>BC1G_01968</i>	Chr3	639,916	642,436	1530	509	57.49	6.24

Abbreviations: AA, amino acids; CDS, coding sequence (bp); MW, molecular weight; pI, isoelectric point.

peroxidase family genes were obtained from *B. cinerea*. The coding sequence (CDS) length of 17 genes was greater than 1000bp, and the CDS length of 14 genes was less than 1000bp. According to the isoelectric point (pI) value, 17 amino acids were acidic and 14 amino acids were alkaline, but this difference was not related to the length of the CDS. The molecular weight of the protein was generally distributed between 20 and 80kDa, with only two exhibiting higher molecular weights of 126 and 136kDa (Table 1).

The amino acid sequence of the products encoded by the peroxidase family genes of *B. cinerea* was phylogenetically analysed with the peroxidase amino acid sequences of *M. oryzae* and *S. cerevisiae*. The peroxidase family genes of *B. cinerea* were divided into nine subfamilies: Class I peroxidase, glutathione peroxidase, animal cyclooxygenase-2, NADPH oxidase (Nox) regulator, peroxiredoxin, alkyl hydroperoxidase D-like protein, catalase, dye-decolorising (Dyp) peroxidase and NADPH oxidase (Nox). *BcPRD11*, *BcPRD10*, *BcCCP2* and

BcCCP1 belong to the class I peroxidase subfamily; *BcGPX3* belongs to the glutathione peroxidase subfamily; *BcPPOA90* and *BcPPOA80* belong to the animal cyclooxygenase subfamily; and *BcNOXR* belongs to the Nox regulator subfamily. *BcPRX1*, *BcPRX3*, *BcPRX4*, *BcPRX7*, *BcPRX8* and *BcPRX9* belong to the peroxiredoxin subfamily; *BcPPOA70* belongs to the alkyl hydroperoxidase D-like protein subfamily; *BcCAT2*, *BcCAT3*, *BcCAT4*, *BcCAT5*, *BcCAT6* and *BcCATA* belong to the catalase subfamily; *BcPRD1*, *BcPRD2*, *BcPRD3*, *BcPRD4*, *BcPRD5*, *BcPRD6*, *BcPRD7*, *BcPRD8* and *BcPRD9* belong to the Dyp peroxidase subfamily; and *BcNOXA* belongs to the NADPH oxidase (Nox) subfamily (Figure 1A).

We established a chromosome distribution map by studying the distribution of peroxidase family members on the chromosomes of *B. cinerea*. The results showed that the 31 peroxidase gene family members were located on 13 of the 18 chromosomes of *B. cinerea* (Figure 1B). Among them, there was one gene on each of chromosomes 7, 14 and 16; two genes on each of chromosomes 1, 4, 6, 9, 10, 11 and 13; three genes on chromosome 2; five genes on chromosome 3 and six genes on chromosome 5.

2.2 | Analysis of Peroxidase Family Gene Structure and Conserved Domains in *B. cinerea*

After obtaining the basic physical and chemical properties and chromosome localisation of the peroxidase family of *B. cinerea*, we then conducted a deep analysis of the gene structure and conserved protein domains of the peroxidase family and visualised the results. In the gene structure, there are obvious differences in the structure of the peroxidase family genes of *B. cinerea*. Among them, the animal cyclooxygenase subfamily gene contains more exons, and the CDS sequence is longer, with *BcPPOA90* having 11 exons and *BcPPOA80* having eight exons, which are the two highest numbers of exons in the *B. cinerea* peroxidase gene family. There are generally fewer exons in genes of the peroxiredoxin subfamily, and the CDS sequence is shorter, with *BcPRX4* having only two exons (Figure 2A). Among the conserved domains, we found that the peroxidase family proteins of *B. cinerea* contained 13 different domains. Among them, proteins with the peroxidase_2 domain were the most common, with *BcPRD2*, *BcPRD3*, *BcPRD4*, *BcPRD5*, *BcPRD6*, *BcPRD7*, *BcPRD8* and *BcPRD9* containing the peroxidase_2 domain (Figure 2B).

2.3 | Expression Analysis of Peroxidase Family Genes in *B. cinerea* in Response to Hyphal Development, H₂O₂ Stress, Infection of *A. thaliana* and Conidium Formation

Peroxidase activity is closely related to oxidation. The peroxidase_2 domain is the most abundant domain in the peroxidase family of *B. cinerea*, so we cultured the wild-type strain B05.10 on potato dextrose agar (PDA) medium containing H₂O₂ and determined the relative colony size in the presence and absence of H₂O₂. The results showed that H₂O₂ inhibited the growth of *B. cinerea*, with the inhibitory effect increasing with increasing H₂O₂ concentration (Figure 3A,B). We performed reverse transcription-quantitative PCR (RT-qPCR)

experiments to detect peroxidase gene expression levels during *B. cinerea* hyphal development, response to H₂O₂ and infection of *Arabidopsis thaliana*. The results showed that the relative expression levels of genes *BcPRD3*, *BcPRD7*, *BcPRD8* and *BcPRD10* were higher under H₂O₂ stress, especially those of the first three genes, and there was also a degree of upregulation of the expression of the genes during hyphal development and infection of *A. thaliana* (Figure 3C). The expression of genes encoding cell-wall-degrading enzymes in wild-type B05.10 and $\Delta BcPRD3$, $\Delta BcPRD7$, $\Delta BcPRD8$ and $\Delta BcPRD10$ knockout mutants was analysed. The results showed that the expression levels of *Bcpg1*, *Bcpgx1*, *Bcpme2*, *Bcpme1* and *Bcpg6* were downregulated to different degrees. We believe that *BcPRD3*, *BcPRD7*, *BcPRD8* and *BcPRD10* positively regulate the expression of genes encoding cell-wall-degrading enzymes, which are related to host cell integrity (Figure S4). Therefore, we speculate that these four genes play an important role in the growth and development of pathogens, response to stress and virulence. During conidial development, the 31 peroxidase genes also showed different expression patterns, with almost all of the four genes, *BcPRD3*, *BcPRD7*, *BcPRD8* and *BcPRD10*, that we focused on being expressed at the highest level at 4 h (Figure 3D). It is speculated, therefore, that the development of conidia may be fastest at 4 h.

2.4 | Effects of Peroxidase Family Genes on the Growth and Development of *B. cinerea*

We had shown that the peroxidase family genes of *B. cinerea* showed different expression patterns during hyphal development. Therefore, we constructed knockout mutants of *BcPRD7* and *BcPRD10* genes and mutants of *BcPRD3* and *BcPRD8* genes to assess their role in the growth and development of the pathogen (Figure S1). We used the wild-type B05.10 strain of *B. cinerea* as a control to observe the colony morphology of the mutants. Mycelia grown for 3 days were stained with calcofluor white (CFW), and the morphology of hyphae (observed by confocal microscopy), conidia and infection structures (both observed by optical microscopy) were studied. The results showed that the colour of the hyphae of wild-type colonies was grey-black, while that of mutant colonies was lighter in colour than that of wild-type colonies (Figure 4A). The average hyphal length of the wild-type strain was 75 μ m, which was smaller than that of the average mutant strain (90 μ m; Figure 4B,D), while the average width of the wild-type hyphae was 10 μ m, which was greater than that of the mutant strain (6–7 μ m; Figure 4B,E). The mean sporulation rate of the wild-type strain was 40×10^8 conidia per dish, while that of the mutants was $4\text{--}5 \times 10^8$ per dish, almost 90% fewer (Figure 4F). The size of individual wild-type conidia was also larger than that of the mutants. The results of the scatter plot showed that the average morphology of the wild-type spores largely had a length and width of around 90 and 50 μ m, respectively, while the mutant spores had typical dimensions of 45 and 40 μ m, respectively (Figure 4C,G). Comparative analysis of the infection structures showed that all strains could produce them, but the formation of the mutant infection structures occurred significantly later in development than those of the wild type, and the number of infection structures was also significantly lower than that of the wild type. At 24 h, in the wild-type strain B05.10, mutants $\Delta BcPRD3$ and $\Delta BcPRD8$ had smaller infection structures, while those in $\Delta BcPRD7$ and $\Delta BcPRD10$ had

5 of 16

FIGURE 1 | Identification, phylogenetic evolution and chromosomal localisation of peroxidase family genes in *Botrytis cinerea*. (A) Phylogenetic tree of peroxidase family genes in *B. cinerea*, *Saccharomyces cerevisiae* and *Magnaporthe oryzae*. (B) Chromosomal localisation of peroxidase family genes in *B. cinerea*.

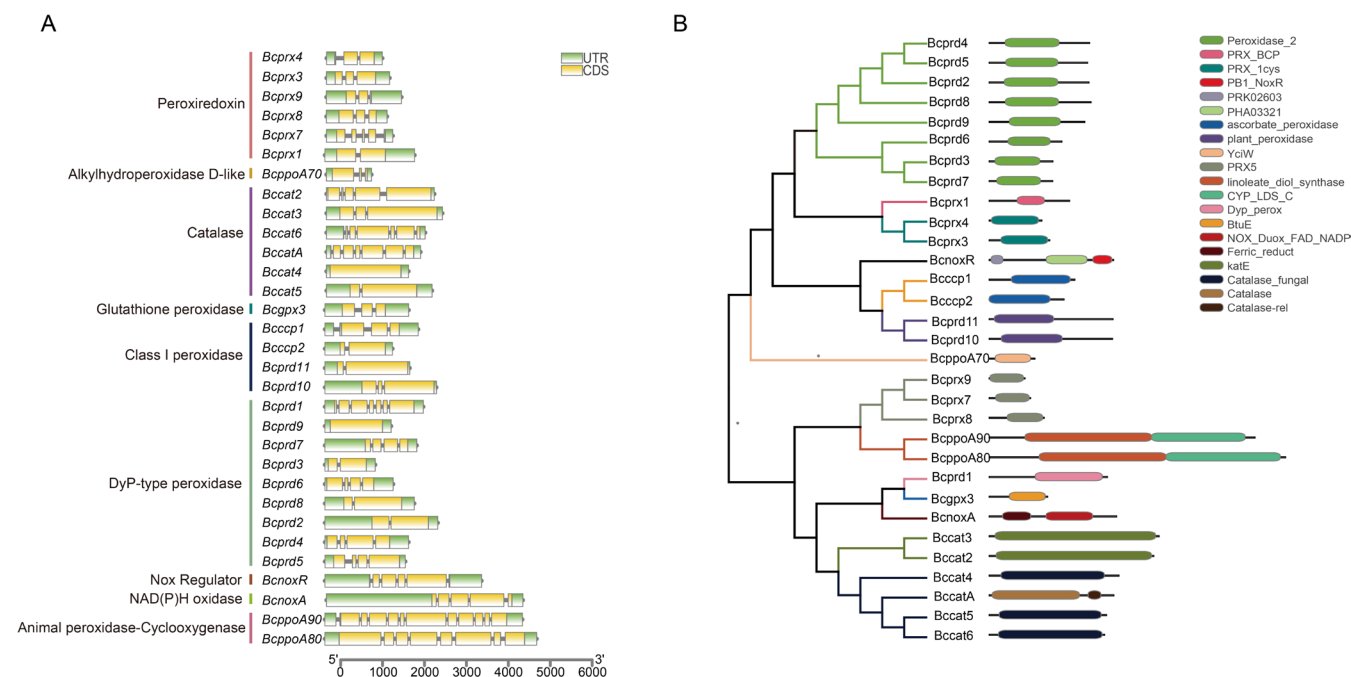


FIGURE 2 | Gene structure and conserved domains of peroxidase family genes in *Botrytis cinerea*. (A) Gene structure of the peroxidase family in *B. cinerea*. CDS, coding sequence; UTR, untranslated region. Size in nucleotides. (B) Conserved domains of peroxidase family genes in *B. cinerea*.

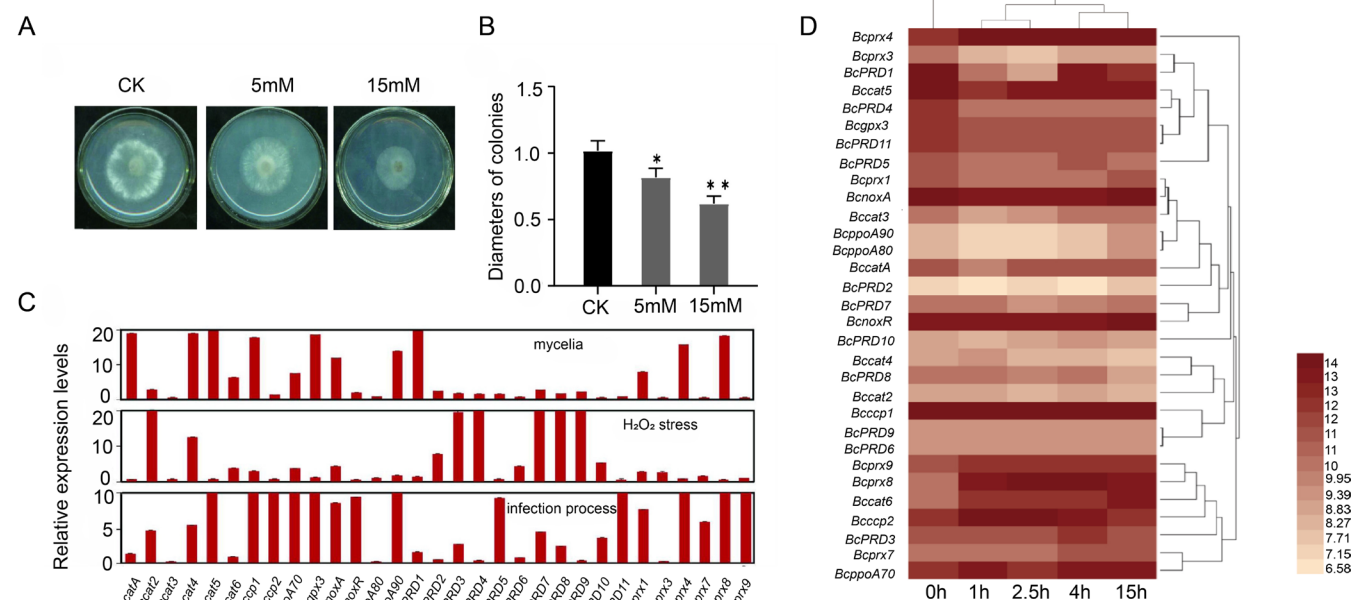


FIGURE 3 | Expression analysis of peroxidase family genes of *Botrytis cinerea* in mycelium and conidia, during the infection process and in response to oxidative stress treatment. (A) Colony morphology of *B. cinerea* under different concentrations of H_2O_2 . CK, negative control (0 mM). (B) Growth rate of *B. cinerea* under different concentrations of H_2O_2 relative to CK (set as 1.0). Significant difference by one-way ANOVA, * $p < 0.05$, ** $p < 0.01$. (C) Expression levels of peroxidase family genes in *B. cinerea* during mycelial development, H_2O_2 stress and infection of *Arabidopsis thaliana*. (D) Expression patterns of peroxidase family genes in conidia of *B. cinerea*.

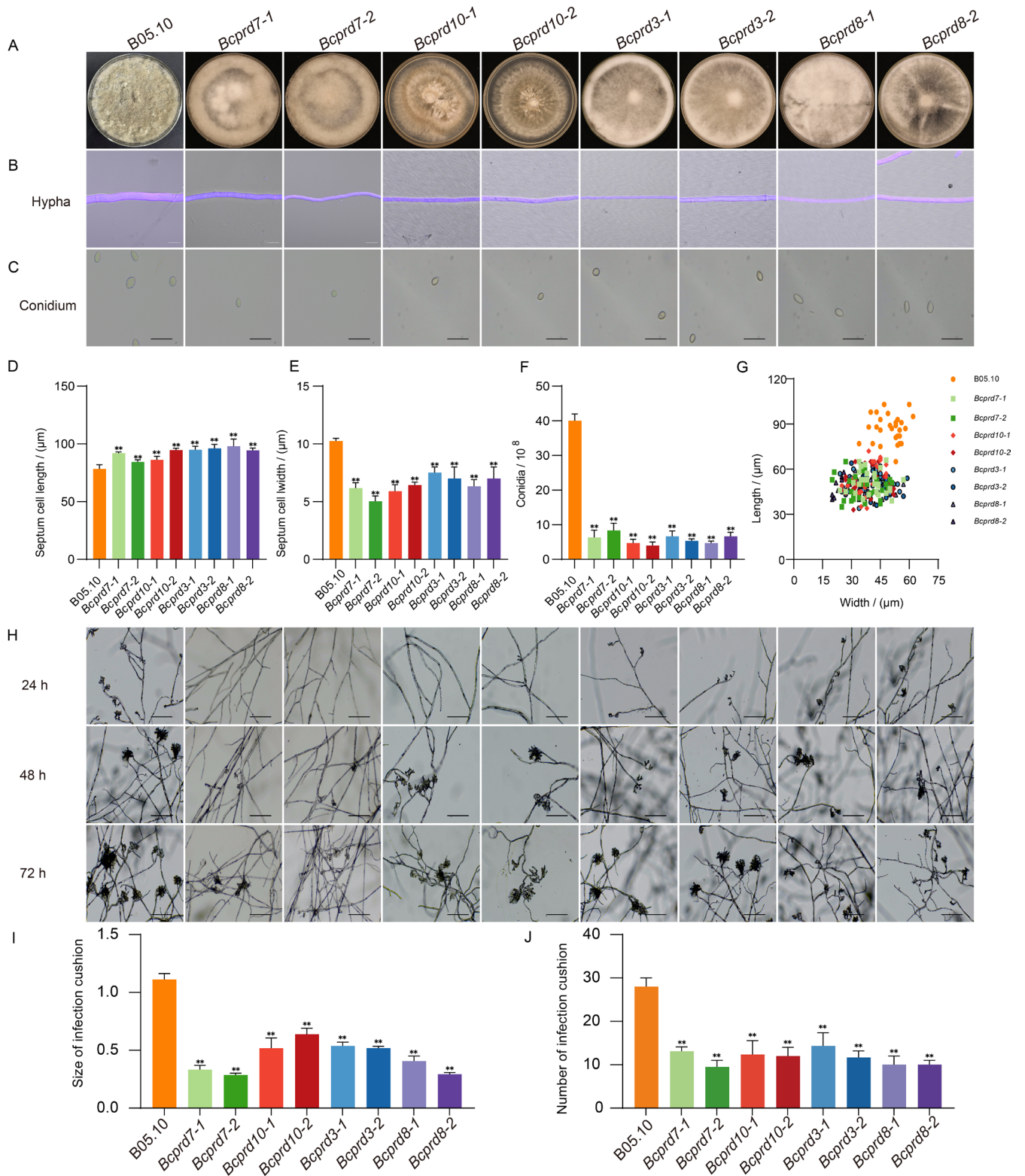


FIGURE 4 | Effects of peroxidase family genes on the growth and development of *Botrytis cinerea*. (A) Surface morphology of wild-type (B05.10) and mutant colonies. (B) Wild-type and mutant hyphal morphology. Bar in the figure is $20\mu\text{m}$. (C) Conidia morphology of wild-type and mutant strains. Bar in the figure is $20\mu\text{m}$. (D) Wild-type and mutant hyphal lengths. (e) Wild-type and mutant hyphal widths. (F) Sporulation rates of wild-type and mutant strains. (G) Length:width ratios of wild-type and mutant conidia. (H) Morphology of wild-type and mutant infection structures at various times after inoculation. Bar in the figure is $20\mu\text{m}$. (I) Relative sizes of the wild-type and mutant infection cushion. (J) Numbers of infection cushion of the wild-type and mutant strains. Significant difference by one-way ANOVA, ** $p < 0.01$.

not yet formed; after 48 and 72 h, the mutants began to exhibit infection structures, but their numbers and sizes were significantly different from the wild type. In terms of number, the wild type reached nearly 30, while the mutant was almost 10 (Figure 4H,I). The infection structures of the mutant were about half the size of the wild-type structures (Figure 4H,I). From these results, we believe that the peroxidase family genes of *B. cinerea* play an important role in the growth and development of the pathogen.

2.5 | Effects of Peroxidase Family Genes of *B. cinerea* on Pathogen Response to Stress

Under oxidative stress treatment, the expression of peroxidase family genes was also affected, indicating that peroxidase family genes could respond to oxidative stress. At the same time, the response to other stress treatments was also assessed. We inoculated wild-type B05.10 and mutant strains at the same growth stage onto potato dextrose agar (PDA) containing NaCl, KCl, H₂O₂, menadione (vitamin K₃), Congo Red or fluconazole, and measured the stress-induced inhibition rate under the different treatments by comparing the treated and control colony diameters (Figure 5A). The results showed that the growth rates of $\Delta BcPRD3$ and $\Delta BcPRD8$ were the slowest while the degree of inhibition was greatest under the NaCl or KCl treatments, with the inhibition level of $\Delta BcPRD7$ being almost the same as that of the wild type, with NaCl actually promoting the growth of $\Delta BcPRD10$ (Figure 5B,C). Under H₂O₂ treatment, the growth rate of $\Delta BcPRD3$ was the lowest, so the degree of inhibition was the highest, while the inhibition level of the wild type was similar to that of the other mutants (Figure 5D). Under menadione treatment, the growth rates of $\Delta BcPRD3$ and $\Delta BcPRD8$ were the lowest and the degree of inhibition was the most obvious. The inhibition level of $\Delta BcPRD7$ was the lowest, being significantly lower than that of the wild type, while the inhibition level of $\Delta BcPRD10-1$ was higher than that of the wild type and $\Delta BcPRD10-2$ was lower than that of the wild type (Figure 5E). In response to treatment with Congo Red, each strain suffered an obvious inhibitory effect, especially $\Delta BcPRD3$, which exhibited the greatest inhibition (Figure 5F). Under fluconazole treatment, the growth rates of $\Delta BcPRD3$ and $\Delta BcPRD8$ were the slowest, and the degree of inhibition was significantly higher than that of the wild type, while those of $\Delta BcPRD7$ and $\Delta BcPRD10$ were lower than that of the wild type (Figure 5G). Therefore, we speculate that the peroxidase family genes of *B. cinerea* can actively respond to osmotic stress and oxidative stress and participate in the regulation of cell integrity, thereby maintaining the stability of fungi in response to changes in the surrounding environment.

2.6 | Effects of Peroxidase Family Genes on the Virulence of *B. cinerea*

The peroxidase family genes of *B. cinerea* exhibited different expression patterns during the infection process of *A. thaliana*, so we then studied their effects on the pathogenicity and virulence of the pathogen. We inoculated the wild-type strain B05.10 and $\Delta BcPRD3$, $\Delta BcPRD7$, $\Delta BcPRD8$ and $\Delta BcPRD10$ mutant strains at the same growth stage onto the surface of *Nicotiana benthamiana* leaves, which were subsequently cultured in a dark and

humid plant culture room for 2 days, after which the lesion areas were recorded in a spectral imager (Figure 6A,C,E,G). The results showed that, except for inoculation with $\Delta BcPRD7$, which did not produce lesions (Figure 6B), all the other strains caused obvious lesions on the leaves, although the lesion area induced by the mutants, at almost 2 cm², was significantly smaller than that caused by the wild type (Figure 6B,D,F,H). Because the virulence of $\Delta BcPRD7$ was much lower than that of the other three mutants, we also made the complemented strain *BcPRD7-C* and did the same observations and analysis. *BcPRD7-C* could produce lesions, but the lesion area was smaller than that of the wild-type (Figure S2a,b). It was found that the distance between successive septa, the width of the hyphae, the sporulation rate, the size of the conidia, the size and number of the infection structures and the stress tolerance of *BcPRD7-C* were all complemented (Figures S5 and S6). We speculate that the virulence of the pathogen was greatly reduced after the knockout of *BcPRD7* or *BcPRD10* genes and the silencing of *BcPRD3* and *BcPRD8* genes, indicating that the peroxidase family genes of *B. cinerea* positively regulate the virulence of the pathogen.

2.7 | Peroxidase Activity Analysis of BcPRD7 Protein in *B. cinerea*

To test the activities of the enzymes encoded by the peroxidase family genes of *B. cinerea*, we selected the BcPRD7 protein, constructed a prokaryotic expression vector, and determined the enzyme amount and enzyme activity curve of this protein. The peroxidase activity of the BcPRD7-6×His non-induced culture and lysate were designated as the controls (CK). The results showed that the peroxidase activity of the BcPRD7-6×His induced culture was 99.5 U/10¹² cells, which was significantly higher than that of the non-induced control (7.3 U/10¹² cells) (Figure 7A). The peroxidase activity of the BcPRD7-6×His induced lysate was 8.7 U/10¹² cells, which was also significantly higher than that of the corresponding control (Figure 7C). The kinetic curve of BcPRD7-6×His showed that the absorbance at 470 nm of the non-induced control culture did not increase after 30 s and reached only 0.15. The value for the induced culture increased from 30 s to 120 s and was 0.55 absorbance units higher than the control (Figure 7B). The kinetic curve showed that the non-induced control lysate did not increase after 30 s and reached only 0.05 whereas the value for the induced lysate increased from 30 s to 120 s and was 0.37 absorbance units higher than the control (Figure 7D). When measuring intracellular ROS levels in wild-type B05.10 and mutant cells, the ROS concentration in the wild-type B05.10 was 140 relative fluorescence units (RFU), which was much higher than that of the mutant, 60–70 RFU (Figure 7E). Therefore, we believe that the BcPRD7 protein exhibits peroxidase activity, which is involved in ROS scavenging.

2.8 | Screening and Identification of BcPRD7-Interacting Proteins in *B. cinerea*

To further explore changes in gene expression and other functions in $\Delta BcPRD7$ and wild-type B05.10, we inoculated potato dextrose broth (PDB) with either strain and cultured them for 12 days, at which point sampling was undertaken for

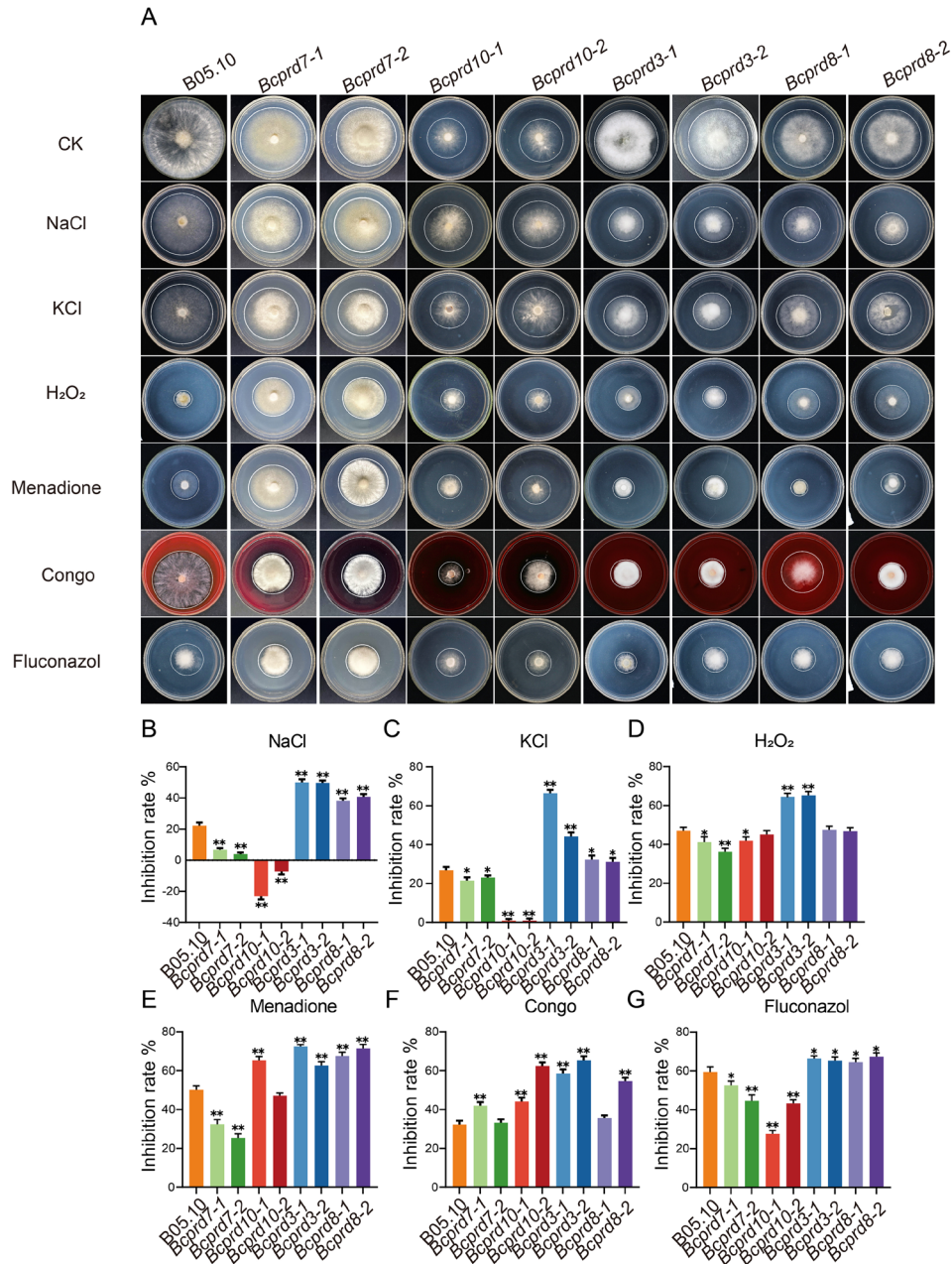


FIGURE 5 | Determination of stress response of peroxidase family genes in *Botrytis cinerea*. (A) Growth of the wild-type (B05.10) and mutant strains under different stresses. CK, negative control. (B) Inhibition rate by NaCl on the wild-type and mutant strains. (C) Inhibition rate by KCl on the wild-type and mutant strains. (D) Inhibition rate by H₂O₂ on the wild-type and mutant strains. (E) Inhibition rate of menadione on the wild-type and mutant strains. (F) Inhibition rate of Congo Red on the wild-type and mutant strains. (G) Inhibition rate of fluconazole on the wild-type and mutant strains. Significant difference by one-way ANOVA, * $p < 0.05$, ** $p < 0.01$.

RNA-sequencing (RNA-Seq) analysis. A total of 7385 differentially expressed genes (DEGs) were identified, of which 1845 genes were significantly upregulated and 1414 genes were significantly downregulated in $\Delta BcPRD7$. We used GO analysis to identify the possible functions or cellular pathways for the DEGs and found that the proteins encoded by the upregulated genes played an important role in oxidoreductase activity, ion transport and mycotoxin synthesis and metabolism, findings that were consistent with results from our research into peroxidase function (Figure 8A). We analysed the metabolic pathways involving DEGs by Kyoto Encyclopedia of Genes and Genomes (KEGG) analysis and found that the DEGs from the $\Delta BcPRD7$

mutant were mainly involved in the biosynthesis of secondary metabolites of *B. cinerea*, of which 43 were significantly upregulated genes. Significantly upregulated genes were also involved in tryptophan metabolism, glycerophospholipid metabolism and starch and sucrose metabolism (Figure 8B). The proteins encoded by downregulated genes were mostly in pathways of carbohydrate metabolism and organic matter catabolism. From the perspective of molecular function, downregulated genes were related to hydrolase activity (Figure S3a). Significantly downregulated genes were involved in starch and sucrose metabolism, mutual conversion of pentose and glucuronic acid and biosynthesis of coenzyme factors (Figure S3b).

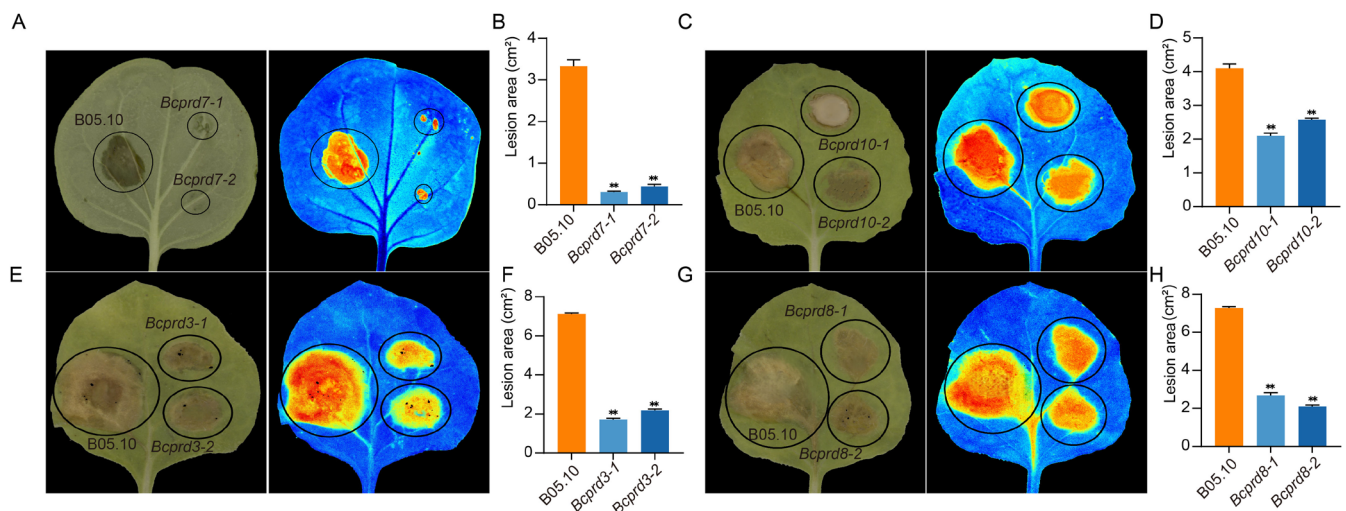


FIGURE 6 | Virulence determination of *Botrytis cinerea* peroxidase family gene mutants on *Nicotiana benthamiana* leaves. (A) Symptoms of *N. benthamiana* infected by the $\Delta BcPRD7$ strain compared to the wild type (B05.10). (B) Lesion area of *N. benthamiana* infected by the $\Delta BcPRD7$ strain. (C) Symptoms of *N. benthamiana* infected by the $\Delta BcPRD10$ strain. (D) Lesion area of *N. benthamiana* infected by the $\Delta BcPRD10$ strain. (E) Symptoms of *N. benthamiana* infected by the $\Delta BcPRD3$ strain. (F) Lesion area of *N. benthamiana* infected by the $\Delta BcPRD3$ strain. (G) Symptoms of *N. benthamiana* infected by the $\Delta BcPRD8$ strain. (H) Lesion area of *N. benthamiana* infected by the $\Delta BcPRD8$ strain. Significant difference by one-way ANOVA, ** $p < 0.01$.

Through GO and KEGG analysis, we found that *BcHEX* has the function of encoding HEX, the main protein in Woronin bodies, which are peroxisome-related organelles that are unique to filamentous fungi. These bodies function to seal the septal pores in response to cellular wounding and prevent the loss of cytoplasm when the fungal hyphae are injured or as they age, which contributes to maintaining the integrity of the hyphae and the stability of the cells. *BcPRD7* has been shown to be related to mycelial growth and development and can regulate cell integrity. We speculated that *BcHEX* might interact with *BcPRD7*. We performed yeast two-hybrid (Y2H) and dual luciferase complementation assays to examine whether *BcHEX* interacts with *BcPRD7*. The results showed that yeast colonies co-transformed with AD-*BcPRD7* and BD-*BcHEX* and BD-*BcPRD7* and AD-*BcHEX* grew normally in the triple-deficient synthetic defined (SD) medium (–Leu/–Trp/–His) and the quadruple-deficient medium (–Leu/–Trp/–His/–Ade), but the yeast colonies co-transformed with other negative control combinations could not grow (Figure 8C). *N. benthamiana* leaves injected with *BcPRD7*-nLUC + *BcHEX*-cLUC and *BcPRD7*-cLUC + *BcHEX*-nLUC showed obvious fluorescent signals under the plant in vivo imaging system, while leaves injected with other *Agrobacterium* combinations showed no fluorescent signals (Figure 8D). Immunoprecipitation (IP) was performed with *BcPRD7* with a FLAG tag. The total protein was incubated with anti-FLAG + Protein A/G for elution and then examined by western blotting. When incubated with anti-FLAG antibodies, both *BcHEX*-Myc + *BcPRD7*-FLAG and *BcPRD7*-FLAG showed specific bands. When incubated with anti-Myc, only *BcHEX*-Myc + *BcPRD7*-FLAG showed specific bands (Figure 8E), indicating that an interaction had occurred between *BcHEX* and *BcPRD7*.

The peroxidase activity of wild-type strain B05.10 was 137 U/g. We transferred the gene *BcHEX* into the B05.10 strain

and measured the enzyme activity again. It was found that the peroxidase activity of *BcHEX*-B05.10 was 168 U/g, so that the enzyme activity had increased by approximately 20% (Figure 8F). Subsequently, we also determined the enzyme activity in $\Delta BcPRD7$ and *BcHEX*- $\Delta BcPRD7$ strains. The results showed that the peroxidase activity of $\Delta BcPRD7$ was 76 U/g, which was significantly lower than that of wild-type B05.10 (Figure 8G). When *BcHEX* was transferred into the mutant, the peroxidase activity of *BcHEX*- $\Delta BcPRD7$ increased to 101 U/g, which was about 30% higher than that of the $\Delta BcPRD7$ strain, showing that *BcHEX* promotes the peroxidase activity of *BcPRD7*.

3 | Discussion

Botrytis cinerea is a typical necrotrophic pathogen and is one of the 10 most economically destructive plant pathogens. It causes grey mould on thousands of plant species, resulting in serious damage to the economic value of these crops. *B. cinerea* usually infects dicotyledonous plants at the early stage of crop development. The infected host organ decays rapidly when the environment is conducive to the maturation of the pathogen, causing large economic losses during transportation and storage. Therefore, in-depth exploration of the virulence genes of *B. cinerea* plays a fundamental role in revealing and understanding the infection mechanism of *B. cinerea*.

The peroxidase gene family is ubiquitous in almost all plants and pathogens. It can catalyse the oxidation of various organic and inorganic substrates by reacting with hydrogen peroxide and similar molecules and has important reductive protection against the detrimental oxidation of host proteins and lipids by ROS. Due to their broad catalytic activity, peroxidases can remove phenolic compounds and peroxides in the

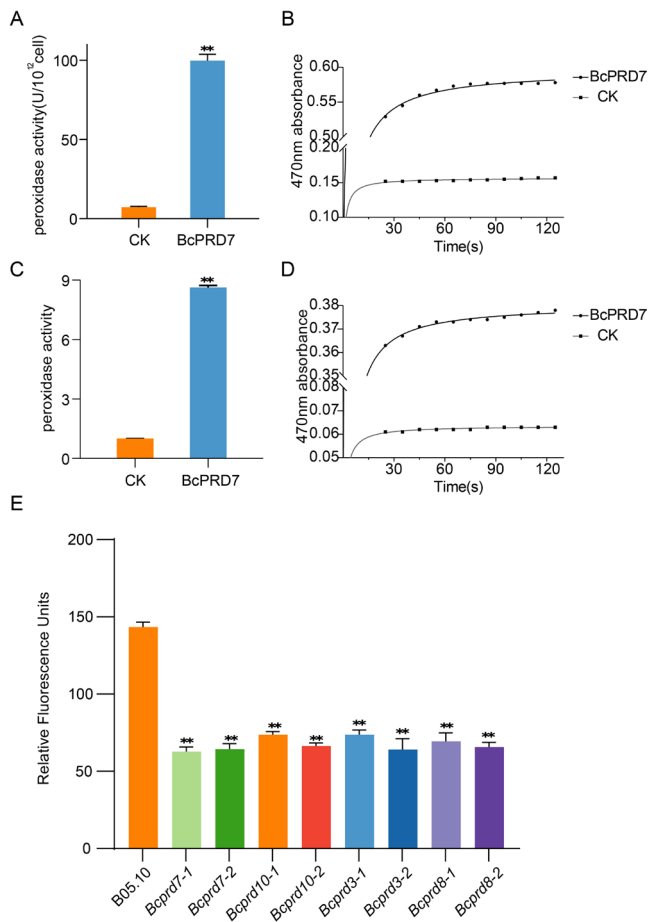


FIGURE 7 | Determination of peroxidase activity of BcPRD7 protein in *Botrytis cinerea*. (A) Peroxidase activity of BcPRD7-6×His-induced culture (U/10¹² cells). CK, non-induced culture. (B) 470nm kinetic curve of BcPRD7-6×His-induced culture. CK, non-induced culture. (C) Peroxidase activity of BcPRD7-6×His-induced lysate. CK, non-induced lysate (set as 1.0). (D) 470nm kinetic curve of BcPRD7-6×His-induced lysate. CK, non-induced lysate. (E) Determination of reactive oxygen species (ROS) levels in Δ BcPRD3, Δ BcPRD7, Δ BcPRD8 and Δ BcPRD10 mutants compared to the wild type (B05.10). Significant difference by one-way ANOVA, ** $p < 0.01$.

degradation of mycotoxins (Monastyrska and Klionsky 2006; Sakai et al. 2006; Meijer et al. 2007). The importance of peroxidases is widely known, and their functional roles have been reported in *P. chrysogenum*, *M. oryzae* and *F. graminearum*. However, there have been few studies on the peroxidase family genes and their specific functions in *B. cinerea*. Therefore, we explored the whole genome of *B. cinerea*. Using bioinformatic methods to screen the *B. cinerea* genome sequence, 31 peroxidase genes of *B. cinerea* were identified and divided into nine subfamilies, containing 15 different domains, reflecting the diversity and functional differentiation within the gene family. In addition, we studied the peroxidase gene family of *B. cinerea* to analyse the physicochemical properties, gene structure and phylogenetic evolution of its members. The peroxidase genes were distributed on 13 chromosomes, and the isoelectric points were between 4.48 and 9.23. By comparison with *S. cerevisiae* and *M. oryzae*, it was found that there are many homologous genes between the peroxidase family of *B. cinerea* and these species. This provides an important tool

with which to understand the evolutionary conservation and function of the peroxidase family in *B. cinerea*.

In addition, we found that the expression of peroxidase family genes in *B. cinerea* varied under different treatments, mutants and stages of development. The expression levels of BcCATA and BcPRD1 were relatively high during mycelial growth, while the expression levels were lower in response to H₂O₂ treatment or infection of *A. thaliana*. The expression levels of BcCAT2, BcPRD3, BcPRD4, BcPRD7, BcPRD8 and BcPRD9 after H₂O₂ treatment were higher than those during hyphal development and infection of *A. thaliana*. The expression levels of BcCCP2, BcPPOA70, BcNOXR, BcPRD5, BcPRD11, BcPRX1, BcPRX7 and BcPRX9 in *A. thaliana* were higher than those following H₂O₂ treatment or during the hyphal development period. In the conidial stage, the highest expression was generally reached at 4 h. Therefore, we speculate that the peroxidase genes of *B. cinerea* may play an important role in hyphal development, conidium formation, virulence and tolerance to abiotic stresses and resistance to biotic stresses.

Studies have reported that peroxidases are involved in the process of pathogen growth and development, confirming our speculation. It has been reported that, after knocking out a peroxidase gene of *F. graminearum*, defects in hyphal and conidial development were observed (Rolke et al. 2004; Giesbert et al. 2008). To investigate this phenomenon, we also constructed a peroxidase gene mutant of *B. cinerea* and analysed the phenotype of the wild-type and mutant strains. It was found that the hyphae of the mutant became thinner, the hyphal cells became longer and the production of conidia was also greatly reduced. The time required to form infection structures increased, and the number of structures decreased; the number and size of *F. graminearum* spores and infection cushions were significantly reduced, and virulence was significantly decreased in the mutant. The results of the *B. cinerea* experiment were consistent with the effects reported earlier for the peroxidase gene of *F. graminearum*. It was clear that the peroxidase gene of *B. cinerea* positively regulates the growth and development of the pathogen, but its mechanism of action is not yet clear, and further research is needed.

Studies have reported that peroxidases are involved in the response of pathogens to stress and regulate the virulence of pathogenic fungi. In yeast, multiple peroxidase genes are induced during the response to oxidative stress (Oliveira et al. 2021). In *F. graminearum*, after knocking out the peroxidase gene, the growth of *F. graminearum* strains on H₂O₂-supplemented medium almost stalled (Guo et al. 2019). We also carried out oxidative stress treatments on peroxidase family gene mutants of *B. cinerea*. It has been reported that fungal cell wall inhibitors could induce ROS in apoptotic cells in yeast cells. With the increase in intracellular ROS concentration, oxidative damage would be caused to cells, and Congo Red would induce ROS production. Therefore, we also supplemented osmotic stress and cell integrity tests. The results showed that the growth rate of Δ BcPRD3 was the slowest and the degree of inhibition was the highest under H₂O₂ treatment, while the inhibition level of the wild type and the other mutant strains was almost the same. The results were similar to the report on *F. graminearum*, but not to the extent

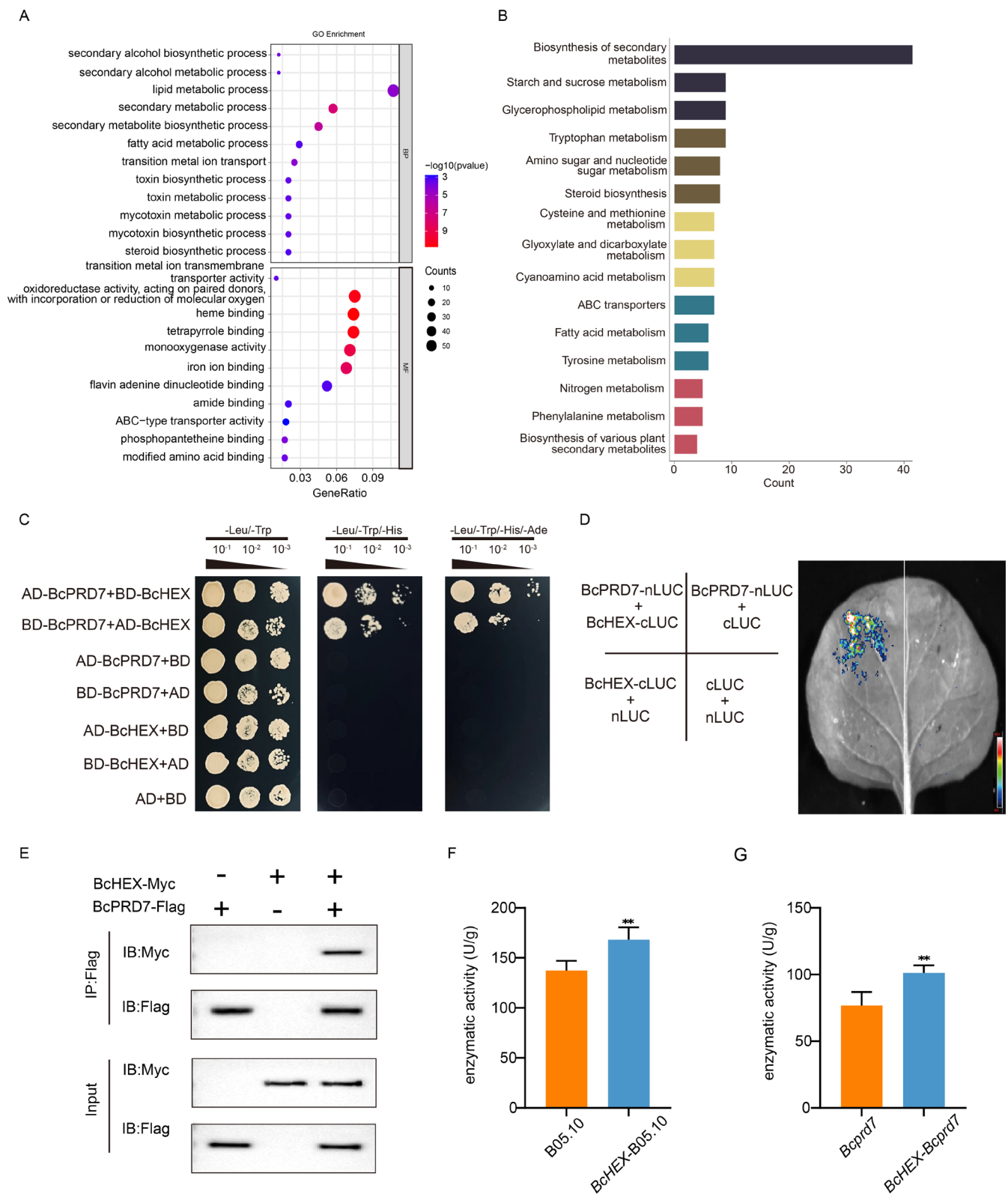


FIGURE 8 | Functional annotation, metabolic pathway analysis and interacting protein verification of upregulated genes of $\Delta BcPRD7$ in *Botrytis cinerea*. (A) Gene Ontology (GO) functional annotation of significantly differentially upregulated genes in $\Delta BcPRD7$ gene knockout mutant. (B) Kyoto Encyclopedia of Genes and Genomes (KEGG) metabolic pathway analysis of significantly upregulated genes in $\Delta BcPRD7$ gene knockout mutant. (C) Yeast two-hybrid verification of BcPRD7 and BcHEX interaction. (D) Luciferase complementation assay verification of BcPRD7 and BcHEX interaction. (E) Co-immunoprecipitation (Co-IP) verification of BcPRD7 and BcHEX interaction. IP, immunoprecipitation; IB, immunoblot. (F) Comparison of peroxidase enzyme activity between B05.10 and BcHEX-B05.10. (G) Comparison of peroxidase enzyme activity between $\Delta BcPRD7$ and BcHEX- $\Delta BcPRD7$. Significant difference by one-way ANOVA, $**p < 0.01$.

that the mutant could not grow; the concentration used in the *Fusarium* study was 20 mM, whereas the concentration in our experiment was only 1 mM, indicating that the concentration of H₂O₂ was directly associated with the growth inhibition of the strain. The results also showed that the strain could respond positively to osmotic stress and oxidative stress and could regulate cell integrity, indicating roles for the peroxidase gene of *B. cinerea* in these responses. Studies have shown that, in *F. graminearum*, the virulence of the peroxidase-gene knockout mutant was greatly reduced compared with the wild type (Lee et al. 2018). In our test results, we inoculated the wild type and mutant strains onto the surface of *N. benthamiana* leaves. The lesion area produced by the mutant strain was much smaller than that achieved by the wild type, with Δ BcPRD7 hardly producing any visible lesions, a finding that was consistent with the reported results and indicating that this peroxidase gene of *B. cinerea* positively regulates the virulence of the pathogen.

Studies have shown that the knockout of peroxidase genes will reduce enzyme activity, greatly reduce oxygen-binding capacity and reduce ion transport capacity. It has also been found in microorganisms that the lack of peroxidase can affect the metabolism of mycotoxins. We explored the function of the peroxidase BcPRD7 in *B. cinerea* and performed RNA-Seq analysis of the *B. cinerea* wild-type strain B05.10 and its BcPRD7 gene knockout mutant Δ BcPRD7. It was found that the DEGs significantly upregulated in the mutant Δ BcPRD7 mainly played roles in oxidase enzyme activity, ion penetration and mycotoxin synthesis and metabolism, findings that were consistent with previous research reports on other fungi. It is speculated that the BcPRD7 gene functions through the peroxisome because, when the BcPRD7 gene is deleted, the function of the peroxisome is weakened, which affects peroxidase activity and thus affects oxygen-binding capacity, ion transport capacity and mycotoxin production and metabolism.

It has been reported that the HEX protein is the main protein in the Woronin body (Yuan et al. 2003). The Woronin body is an organelle unique to filamentous fungi, being a specialised peroxisome located near the edge of the cell or the septa of the hyphae. Its function is to maintain the integrity of the cell structure when the cell is damaged (Tang et al. 2020). It has been found that the knockout of the *HEX1* gene in *Neurospora crassa* can lead to the leakage of cytoplasm following cell lysis (Jedd and Chua 2000). The hyphal morphology of a *HEX1* gene deletion mutant of *M. oryzae* changed, and the ability of appressoria to penetrate or colonise host cells decreased (Xu et al. 2021). We confirmed the interaction between BcPRD7 and BcHEX, so it is speculated that the BcPRD7 protein may affect the function of the Woronin body by interacting with BcHEX, thus participating in the growth and development of pathogens, their virulence and involvement in the regulation of cell integrity.

We identified 31 peroxidase family genes in *B. cinerea*, which were distributed across 13 chromosomes and could be divided into nine subfamilies. The 31 peroxidase family proteins of *B. cinerea* contained 15 different domains and showed different expression patterns in conidia, hyphae, response to H₂O₂ stress and the infection period of the pathogen. It was clear that the peroxidase genes of *B. cinerea* positively regulated the growth and

virulence of *B. cinerea* and participated in the response of the pathogen to osmotic stress, oxidative stress and the regulation of cell integrity. The interaction between BcPRD7 and BcHEX protein was clarified. The current in-depth study of the peroxidase gene of *B. cinerea* is of great significance for controlling the grey mould disease. In future research, we will further explore the mechanism of action of BcPRD7 and the Woronin body and lay the foundation for elucidating the functions of the peroxidase family genes in *B. cinerea*.

4 | Experimental Procedures

4.1 | Fungal and Plant Material

The *B. cinerea* wild-type B05.10, mutants Δ BcPRD3, Δ BcPRD7, Δ BcPRD8 and Δ BcPRD10 and *N. benthamiana* were preserved and provided by Hebei Key Laboratory of Plant Physiology and Molecular Pathology.

4.2 | Gene Structure Analysis of the Peroxidase Family in *B. cinerea*

The amino acid sequences of the peroxidase family of three fungal species, *B. cinerea*, *S. cerevisiae* and *M. oryzae*, were downloaded from the fungal peroxidase gene database (<http://peroxiDase.riceblast.snu.ac.kr>). MEGA software was used for amino acid sequence alignment, and the phylogenetic tree was constructed by the neighbour-joining method. The development tree was visualised using Evolview (<http://www.evolgenius.info/evolview>).

The Ensembl Fungi (<http://fungi.ensembl.org/>) database was queried to obtain the chromosome length of *B. cinerea* and the gene location information on the genes of the peroxidase family. Using TBtools software, chromosome localisation visualisation was performed to obtain the chromosome localisation map of peroxidase family genes. The DNA sequence information of the *B. cinerea* peroxidase family genes was obtained from the Ensembl Fungi database. TBtools software was used to visualise the genetic structure. The amino acid sequences of the proteins encoded by the 31 peroxidase family genes in *B. cinerea* were analysed by using the online website SMART (<http://smart.embl-heidelberg.de/>). TBtools software was used to visualise the protein domains.

4.3 | Gene Expression Analysis of Peroxidase Family Genes in *B. cinerea*

From the GEO (<https://www.ncbi.nlm.nih.gov/geo/>) database, the expression profile data of the development period of *B. cinerea* hyphae and conidia was downloaded, and Heml software was used to analyse the expression pattern of peroxidase family genes during the germination of *B. cinerea* conidia and the growth of hyphae.

H₂O₂ at final concentrations of 0, 5, or 15 mM was added to the PDA, and the *B. cinerea* B05.10 strain was inoculated onto the medium and cultured in the dark at 25°C. The growth of

B. cinerea was observed on solid medium for 3 days. H₂O₂ at a final working concentration of 0 (control, CK) or 5 mM was added to PDB, and the *B. cinerea* B05.10 strain was inoculated. After 7 days, the samples in the liquid medium were collected and stored at −80°C. The specific primers of *B. cinerea* peroxidase family genes (Table S1) were used to extract the RNA of *B. cinerea* grown under 0 or 5 mM H₂O₂ stress treatment, which was reverse-transcribed into cDNA as a template for qPCR detection. Using the *BcACTA* actin gene as the internal reference gene, the relative expression levels of each gene were analysed by the comparative 2^{−ΔΔCt} value method. One-way analysis of variance was performed on the data using GraphPad Prism software. **p* < 0.05, ***p* < 0.01.

Mycelial plugs (6 mm diameter) from 7-day-old *B. cinerea* B05.10 cultures were inoculated onto the adaxial surface of healthy *Arabidopsis* leaves and cultured at 25°C in the dark for 5 days. The mycelial RNA was extracted and reverse-transcribed into cDNA. The cDNA template was used for qPCR detection by using the specific primers for the peroxidase family genes of *B. cinerea* (Table S1), with *BcACTA* as the internal reference gene. The relative expression levels of each gene were analysed by the comparative 2^{−ΔΔCt} value method.

Seven-day-old cultures of *B. cinerea* B05.10 and Δ*BcPRD3*, Δ*BcPRD7*, Δ*BcPRD8* and Δ*BcPRD10* mutants were used to extract mycelial RNA, which was reverse-transcribed into cDNA. The expression of cell-wall-degrading enzyme genes was detected by qPCR using cDNA templates, with *BcACTA* as the internal reference gene. The relative expression levels of each gene were analysed by the comparative 2^{−ΔΔCt} value method.

4.4 | Phenotypic Analysis of Δ*BcPRD3*, Δ*BcPRD7*, Δ*BcPRD8* and Δ*BcPRD10* Mutants

Coverslips were obliquely inserted into the medium of cultures of the wild-type B05.10 and corresponding mutant strains on PDA plates. After 3 days of culture, the coverslips were removed, 50 μL CFW (10 μg/mL) stain solution was added dropwise, and the coverslips were placed in the dark for 30 min. Confocal fluorescence microscopy (Solarbio) was used to observe and count the length and width of the hyphae.

Studies on the infection cushions of these strains followed the same procedure, except that three coverslips were inserted. One coverslip was removed every other day and observed under an optical microscope, and the shape, size and number of infection cushions were recorded. The wild-type B05.10 and mutant strains grown on PDA plates under the same culture conditions were washed with 20 mL double-distilled water, and the conidia were collected, with the number of conidia being counted (to determine sporulation rate) under an optical microscope.

4.5 | Determination of Stress Response of Δ*BcPRD3*, Δ*BcPRD7*, Δ*BcPRD8* and Δ*BcPRD10* Mutants

The wild-type strain B05.10 and mutant strains were inoculated onto PDA containing 0.8 M NaCl, 0.8 M KCl, 10 mM H₂O₂,

250 μM menadione, 2 mg/mL Congo Red or 10 μg/mL fluconazole. The sensitivity of each strain to osmotic stressors, oxidative stressors and inhibitors of cell walls and cell membranes was determined. After 4 days of culture, the growth diameter of the colonies of each strain was measured, and the inhibition rate (relative to the wild type) was calculated.

4.6 | Virulence of Δ*BcPRD3*, Δ*BcPRD7*, Δ*BcPRD8* and Δ*BcPRD10* Mutants

Plugs (6 mm diameter) were punched from 7-day-old cultures of wild-type B05.10 and mutant strains on PDA using a sterile hole punch and were used to inoculate fresh PDA plates of the same growth environment and time. After adding 30 μL Tween 20 to the surface of *N. benthamiana* leaves, the fungal plate was inoculated onto the top surface of the leaves. After 2 days of culture in the dark under high-humidity conditions, the inoculated leaves were analysed by a multispectral imager, and the lesion area was measured.

4.7 | Peroxidase Activity Analysis of the BcPRD7 Protein in *B. cinerea*

The constructed *BcPRD7*-28a plasmid was transformed into *Escherichia coli* BL21. A total of 200 μL of the suspension of *BcPRD7*-28a in BL21 was inoculated into 20 mL LB medium containing kanamycin (1% wt/vol) at 37°C in a shaking incubator (220 rpm) to OD₆₀₀ ≈ 0.6, when 0.1 mM isopropyl β-D-1-thiogalactopyranoside (IPTG) was added before incubating at 28°C and 200 rpm for 6 h to induce the expression of BcPRD7-6×His recombinant protein, after which the OD₆₀₀ value of the bacterial culture was measured. The cells in an ice-water mixture were lysed ultrasonically. The ultrasonic power was 200 W, each period of ultrasound was 3 s, the interval between exposures was 5 s, and the cells were lysed for a total of 5 min. The peroxidase activity of the induced BcPRD7 culture and lysate was detected by the Peroxidase Detection Kit (Solarbio). The ROS levels of wild-type B05.10 and mutants Δ*BcPRD3*, Δ*BcPRD7*, Δ*BcPRD8* and Δ*BcPRD10* were determined using an ROS assay kit, and the fluorescence intensity value was recorded.

4.8 | Validation of BcPRD7-Interacting Proteins in *B. cinerea*

The constructed AD-*BcPRD7* plasmid (1 μg) was combined with 1 μg BD-*BcHEX* or BD-*BcPRD7* plasmids. The 1 μg BD-*BcPRD7* plasmid was combined with 1 μg AD-*BcHEX*, and a negative control combination was set up. Each plasmid combination was transformed into competent yeast cells, plated onto double-deficient (−Leu/−Trp) medium and cultured at 28°C for 2–3 days. The yeast clones that grew well on the double-deficient medium were selected for gradient dilution, and the growth state was observed on the double-deficient (−Leu/−Trp), triple-deficient (−Leu/−Trp/−His) and quadruple-deficient (−Leu/−Trp/−His/−Ade) medium.

The constructed luciferase complementary vector was transformed into competent *Agrobacterium tumefaciens* GV3101

cells, and single clones were selected for PCR identification. The cells were resuspended in a 10mM MgCl₂ solution containing 100mM acetosyringone two or three times, and the OD₆₀₀ of the bacterial solution was adjusted to 2.0. The *Agrobacterium* suspension was injected into *N. benthamiana* leaves. After 48 h, the leaves were treated with D-luciferin containing 1 mM firefly substrate, and fluorescence detection was performed using a plant in vivo imaging system.

The constructed *BcHEX*-Myc, *BcPRD7*-FLAG vectors were transformed into competent *A. tumefaciens* GV3101 cells, and *N. benthamiana* transformants were obtained by *A. tumefaciens*-mediated transformation (ATMT). The proteins were extracted and immunoprecipitated using magnetic beads. The co-immunoprecipitation (Co-IP) products were analysed by SDS-PAGE and western blotting.

We transformed the constructed *BcHEX* vector into competent *A. tumefaciens* GV3101 cells and then *BcHEX* was transformed into B05.10 and Δ*BcPRD7* by ATMT. The peroxidase activity of the two transformants was determined, and the enzyme activity of the strains without the *BcHEX* sequence was compared to determine the specific changes in enzyme activity. The activity of peroxidase was calculated by using the Peroxidase Activity Kit (Solarbio), based on the rate of change of OD₄₇₀.

Acknowledgements

This study was supported by the Science & Technology Program of Hebei (23567601H), National Natural Science Foundation of China (32072369), Natural Science Foundation of Hebei Province (C2022204040), Research Project of Science and Technology in Colleges and Universities of Hebei Province (BJK2022006) and Baoding Science and Technology Project Program (2472P005).

Conflicts of Interest

The authors declare no conflicts of interest.

Data Availability Statement

The authors confirm that the data supporting the findings of this study are available within the article.

References

- Auh, C. K., and T. M. Murphy. 1995. "Plasma Membrane Redox Enzyme Is Involved in the Synthesis of O₂ and H₂O₂ by *Phytophthora* Elicitor-Stimulated Rose Cells." *Plant Physiology* 107: 1241–1247.
- Bi, K., Y. Liang, T. Mengiste, and A. Sharon. 2023. "Killing Softly: A Roadmap of *Botrytis cinerea* Pathogenicity." *Trends in Plant Science* 28: 211–222.
- Chen, J., J. Luo, Y. Wang, et al. 2021. "Suppression of Female Fertility in *Aedes aegypti* With a CRISPR-Targeted Male-Sterile Mutation." *Proceedings of the National Academy of Sciences of the United States of America* 118: e2105075118.
- Dean, R., J. A. Van Kan, Z. A. Pretorius, et al. 2012. "The Top 10 Fungal Pathogens in Molecular Plant Pathology." *Molecular Plant Pathology* 13: 414–430.
- Giesbert, S., T. Schurg, S. Scheele, and P. Tudzynski. 2008. "The NADPH Oxidase Cpnx1 Is Required for Full Pathogenicity of the Ergot Fungus *Claviceps purpurea*." *Molecular Plant Pathology* 9: 317–327.

- Glazebrook, J. 2005. "Contrasting Mechanisms of Defense Against Biotrophic and Necrotrophic Pathogens." *Annual Review of Phytopathology* 43: 205–227.
- Guo, Y., S. Yao, T. Yuan, Y. Wang, D. Zhang, and W. Tang. 2019. "The Spatiotemporal Control of KatG2 Catalase-Peroxidase Contributes to the Invasiveness of *Fusarium graminearum* in Host Plants." *Molecular Plant Pathology* 20: 685–700.
- He, A., J. M. Dean, and I. J. Lodhi. 2021. "Peroxisomes as Cellular Adaptors to Metabolic and Environmental Stress." *Trends in Cell Biology* 31: 656–670.
- Heller, J., and P. Tudzynski. 2011. "Reactive Oxygen Species in Phytopathogenic Fungi: Signaling, Development, and Disease." *Annual Review of Phytopathology* 49: 369–390.
- Hodaei, M., M. Rahimmalek, A. Arzani, et al. 2018. "The Effect of Water Stress on Phytochemical Accumulation, Bioactive Compounds and Expression of Key Genes Involved in Flavonoid Biosynthesis in *Chrysanthemum morifolium* L." *Industrial Crops and Products* 12: 295–304.
- Jedd, G., and N. H. Chua. 2000. "A New Self-Assembled Peroxisomal Vesicle Required for Efficient Resealing of the Plasma Membrane." *Nature Cell Biology* 2: 226–231.
- Kiel, J. A., I. J. van der Klei, M. A. van den Berg, R. A. Bovenberg, and M. Veenhuis. 2005. "Overproduction of a Single Protein, *Pc-Pex11p*, Results in 2-Fold Enhanced Penicillin Production by *Penicillium chrysogenum*." *Fungal Genetics and Biology* 42: 154–164.
- Lee, D., N. K. Lal, Z.-J. D. Lin, et al. 2020. "Regulation of Reactive Oxygen Species During Plant Immunity Through Phosphorylation and Ubiquitination of RBOHD." *Nature Communications* 11: 1838.
- Lee, Y., H. Son, J. Y. Shin, G. J. Choi, and Y. W. Lee. 2018. "Genome-Wide Functional Characterization of Putative Peroxidases in the Head Blight Fungus *Fusarium graminearum*." *Molecular Plant Pathology* 19: 715–730.
- Lodhi, I. J., and C. F. Semenkovich. 2014. "Peroxisomes: A Nexus for Lipid Metabolism and Cellular Signaling." *Cell Metabolism* 19: 380–392.
- Mahalingam, S. S., N. Shukla, J. C. Farré, K. Zientara-Rytter, and S. Subramani. 2021. "Balancing the Opposing Principles That Govern Peroxisome Homeostasis." *Trends in Biochemical Sciences* 46: 200–212.
- Meijer, W. H., I. J. van der Klei, M. Veenhuis, and J. A. Kiel. 2007. "ATG Genes Involved in Non-Selective Autophagy are Conserved From Yeast to Man, but the Selective Cvt and Pexophagy Pathways Also Require Organism-Specific Genes." *Autophagy* 3: 106–116.
- Monastyrska, I., and D. J. Klionsky. 2006. "Autophagy in Organelle Homeostasis: Peroxisome Turnover." *Molecular Aspects of Medicine* 27: 483–494.
- Octavia, Y., C. G. Tocchetti, K. L. Gabrielson, S. Janssens, H. J. Crijns, and A. L. Moens. 2012. "Doxorubicin-Induced Cardiomyopathy: From Molecular Mechanisms to Therapeutic Strategies." *Journal of Molecular and Cellular Cardiology* 52: 1213–1225.
- Oliveira, F. K., L. O. Santos, and J. G. Buffon. 2021. "Mechanism of Action, Sources, and Application of Peroxidases." *Food Research International* 143: 110266.
- Piasecka, A., N. Jedrzejczak-Rey, and P. Bednarek. 2015. "Secondary Metabolites in Plant Innate Immunity: Conserved Function of Divergent Chemicals." *New Phytologist* 206: 948–964.
- Platta, H. W., and R. Erdmann. 2007. "Peroxisomal Dynamics." *Trends in Cell Biology* 17: 474–484.
- Rolke, Y., S. Liu, T. Quidde, et al. 2004. "Functional Analysis of H₂O₂-Generating Systems in *Botrytis cinerea*: The Major Cu-Zn-Superoxide Dismutase (BCSOD1) Contributes to Virulence on French Bean, Whereas a Glucose Oxidase (BCGOD1) is Dispensable." *Molecular Plant Pathology* 5: 17–27.

- Sakai, Y., M. Oku, I. J. van der Klei, and J. A. Kiel. 2006. "Pexophagy: Autophagic Degradation of Peroxisomes." *Biochimica et Biophysica Acta (BBA) - Molecular Cell Research* 1763: 1767–1775.
- Shai, N., E. Yifrach, C. W. T. van Roermund, et al. 2018. "Systematic Mapping of Contact Sites Reveals Tethers and a Function for the Peroxisome-Mitochondria Contact." *Nature Communications* 9: 1761.
- Shaw, W. R., E. Teodori, S. N. Mitchell, et al. 2014. "Mating Activates the Heme Peroxidase HPX15 in the Sperm Storage Organ to Ensure Fertility in *Anopheles gambiae*." *Proceedings of the National Academy of Sciences of the United States of America* 111: 5854–5859.
- Shigeto, J., G. Y. Kiyonaga, K. Fujita, et al. 2013. "Putative Cationic Cell-Wall-Bound Peroxidase Homologues in *Arabidopsis*, *AtPrx2*, *AtPrx25*, and *AtPrx71*, are Involved in Lignification." *Journal of Agricultural and Food Chemistry* 61: 3781–3788.
- Staats, M., P. van Baarlen, and J. A. Kan. 2005. "Molecular Phylogeny of the Plant Pathogenic Genus *Botrytis* and the Evolution of Host Specificity." *Molecular Biology and Evolution* 22: 333–346.
- Stefanato, F. L., E. Abou-Mansour, A. Buchala, et al. 2009. "The ABC Transporter BcatrB From *Botrytis cinerea* Exports Camalexin and is a Virulence Factor on *Arabidopsis thaliana*." *Plant Journal* 58: 499–510.
- Tang, G., Y. Shang, S. Li, and C. Wang. 2020. "MrHex1 is Required for Woronin Body Formation, Fungal Development and Virulence in *Metarhizium robertsii*." *Journal of Fungi* 6: 172.
- Torres, M. A., J. L. Dangl, and J. D. Jones. 2002. "*Arabidopsis* gp91phox Homologues *AtrbohD* and *AtrbohF* Are Required for Accumulation of Reactive Oxygen Intermediates in the Plant Defense Response." *Proceedings of the National Academy of Sciences of the United States of America* 99: 517–522.
- Vela-Corcía, D., D. Aditya Srivastava, A. Dafa-Berger, N. Rotem, O. Barda, and M. Levy. 2019. "MFS Transporter From *Botrytis cinerea* Provides Tolerance to Glucosinolate-Breakdown Products and is Required for Pathogenicity." *Nature Communications* 10: 2886.
- Wang, J., Z. Zhang, Y. Wang, et al. 2013. "PTS1 Peroxisomal Import Pathway Plays Shared and Distinct Roles to PTS2 Pathway in Development and Pathogenicity of *Magnaporthe oryzae*." *PLoS One* 8: e55554.
- Wang, X., S. Yang, B. Li, et al. 2024. "Exogenous 5-Aminolevulinic Acid Enhanced Saline-Alkali Tolerance in Pepper Seedlings by Regulating Photosynthesis, Oxidative Damage, and Glutathione Metabolism." *Plant Cell Reports* 43: 267.
- Williamson, B., B. Tudzynski, P. Tudzynski, et al. 2007. "*Botrytis cinerea*: The Cause of Grey Mould Disease." *Molecular Plant Pathology* 8: 561–580.
- Xu, R., Y. B. Li, C. Liu, et al. 2021. "Twintin Regulates Actin Assembly and Hexagonal Peroxisome 1 (Hex1) Localization in the Pathogenesis of Rice Blast Fungus *Magnaporthe oryzae*." *Molecular Plant Pathology* 22: 1641–1655.
- Yang, Q., J. Yang, Y. Wang, et al. 2022. "Broad-Spectrum Chemicals Block ROS Detoxification to Prevent Plant Fungal Invasion." *Current Biology* 32: 3886–3897.
- You, Y., and J. A. van Kan. 2021. "Bitter and Sweet Make Tomato Hard to (b) Eat." *New Phytologist* 230: 90–100.
- Yuan, J. G., P. Yuan, G. Jedd, et al. 2003. "AHEX-1crystal Lattice Required for Woronin Body Function in *Neurospora crassa*." *Nature Structural and Molecular Biology* 10: 264–270.

Supporting Information

Additional supporting information can be found online in the Supporting Information section.